Suboxide/subnitride formation on Ta masks during magnetic material etching by reactive plasmas

Cite as: J. Vac. Sci. Technol. A **33**, 040602 (2015); https://doi.org/10.1116/1.4919925
Submitted: 30 March 2015 . Accepted: 27 April 2015 . Published Online: 06 May 2015

Hu Li, Yu Muraki, Kazuhiro Karahashi, and Satoshi Hamaguchi

Suboxide/subnitride formation on Ta masks during magnetic material etching by reactive plasmas

Hu Li, Yu Muraki, Kazuhiro Karahashi, and Satoshi Hamaguchi[a)]
Center for Atomic and Molecular Technologies, Osaka University, Yamadaoka 2-1, Suita 565-0871, Japan

(Received 30 March 2015; accepted 27 April 2015; published 6 May 2015)

Etching characteristics of tantalum (Ta) masks used in magnetoresistive random-access memory etching processes by carbon monoxide and ammonium (CO/NH_3) or methanol (CH_3OH) plasmas have been examined by mass-selected ion beam experiments with *in-situ* surface analyses. It has been suggested in earlier studies that etching of magnetic materials, i.e., Fe, Ni, Co, and their alloys, by such plasmas is mostly due to physical sputtering and etch selectivity of the process arises from etch resistance (i.e., low-sputtering yield) of the hard mask materials such as Ta. In this study, it is shown that, during Ta etching by energetic CO^+ or N^+ ions, suboxides or subnitrides are formed on the Ta surface, which reduces the apparent sputtering yield of Ta. It is also shown that the sputtering yield of Ta by energetic CO^+ or N^+ ions has a strong dependence on the angle of ion incidence, which suggests a correlation between the sputtering yield and the oxidation states of Ta in the suboxide or subnitride; the higher the oxidation state of Ta, the lower is the sputtering yield. These data account for the observed etch selectivity by CO/NH_3 and CH_3OH plasmas. © *2015 American Vacuum Society*. [http://dx.doi.org/10.1116/1.4919925]

I. INTRODUCTION

Magnetoresistive random-access memory (MRAM) is considered as one of the most promising nonvolatile memory device technologies. MRAM devices of very large-scale integration, if realized, could replace dynamic random-access memories of computer chips and reduce their energy consumption significantly.[1–4] As the device technologies of MRAMs have advanced, mass-production technologies for MRAM devices have also been extensively studied. Currently, the miniaturization of MRAM devices is limited by the lack of nanoscale patterning technologies for magnetic metals of MRAM stacks. Although ion milling has been used for MRAM patterning, it is based on physical sputtering and can be used only for low-density patterning of metal surfaces because of poor selectivity against mask materials, metal redeposition on the sidewalls, and metal damages.

As opposed to physical sputtering, reactive ion etching (RIE) may be used to avoid such problems by forming volatile species containing the surface materials, which may enable highly dense patterning of thin films if right surface chemical reactions forming such volatile species are available. For most semiconductor materials such as Si, RIE has been extensively used in their micro and nanoscale patterning. Also, for magnetic metals, there have been various attempts to devise efficient RIE processes for their small-scale patterning. For example, etching of magnetic materials by Cl_2 based plasmas has been proposed,[5–8] but under typical conditions of chlorine etching of magnetic materials, metal chlorides are not volatile and corrosion occurs on etched metal surfaces.

In an attempt to generate volatile metal carbonyls such as tetracarbonylnickel $Ni(CO)_4$ as etch products, reactive plasmas made from carbon monoxide and ammonium (CO/NH_3)[6,9–14] or methanol (CH_3OH)[15–17] have been also proposed as RIE processes for magnetic metals. It has been shown that, with such reactive plasmas combined with hard masks made of Ti or Ta, high etch rates and high selectivity can be achieved. However, despite its initial attempt to generate metal carbonyls in these processes, some studies have indicated that no metal carbonyls are generated to a significant degree and etching takes place essentially by physical sputtering of magnetic materials with simultaneous oxidation or nitridation of the mask materials.[10] These results infer that the observed selectivity in a CO/NH_3 or CH_3OH plasma etching process is attributed to the low sputtering yield of the hard mask, rather than enhanced sputtering yield of magnetic materials.

The goal of this study is, therefore, to understand etching characteristics of Ta, which is a common hard mask material used in MRAM etching processes, by energetic incidence of CO^+ and N^+ ions, which are common ionic species of CO/NH_3 or CH_3OH plasmas. For comparison, sputtering yields of Ta, Ta_2O_5, and TaN by energetic Ar^+ ions are also obtained as functions of the incident energy in this study. To understand faceting characteristics of a Ta hard mask, we have also examined the sputtering yield of Ta and the chemical compositions of beam irradiated Ta surfaces as functions of the ion incident angle. As we shall discuss later, there seems a correlation between the chemical compositions of the beam irradiated Ta surface and its sputtering yield.

II. EXPERIMENTAL METHODS

In this study, a mass-selected ion beam system[18–25] was used to investigate Ta etching processes. The beam system allows only desired ions with specified incident energy to be injected into a sample surface. In this system, ions are

[a)]Electronic mail: hamaguch@ppl.eng.osaka-u.ac.jp

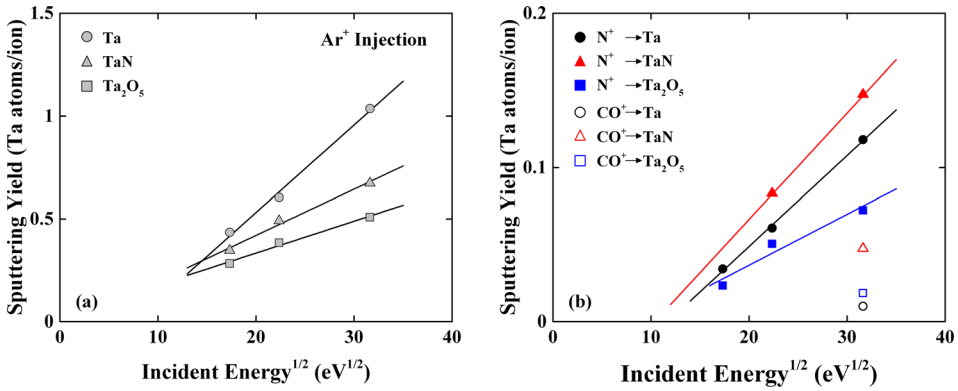

FIG. 1. (Color online) Sputtering yields of Ta, TaN, and Ta_2O_5 by (a) Ar^+ ion beams and (b) N^+ and CO^+ ion beams at normal incidence as functions of the incident ion energy.

generated in a plasma formed in the ion source and specific ions such as Ar^+, CO^+, or N^+ relevant for this study are selected by the mass analyzing magnet. Ions thus extracted and selected are then injected into the surface of a sample set in the ultrahigh vacuum chamber, where the gas pressure is typically kept in the range of 10^{-8} Pa. With a rotatable sample holder, the ion incident angle can be varied from 0° (i.e., normal incidence) to about 75°. The ion beam current is measured by a Faraday cup. Details of this ion beam system may be found in Ref. 25.

The sample used in each experiment of this study was a $1.5 \times 1.5\,cm^2$ Si substrate whose top surface is coated with sputter-deposited Ta, Ta_2O_5, or TaN. Prior to Ar^+, CO^+, or N^+ beam injection, the sample surface was cleaned by 1000 eV Ar^+ ion injection. The sputtering yield is defined as the number of Ta atoms removed from the surface per ion incidence and was evaluated from the etched depth measured by a surface profiler (Dektak3ST) and the ion dose. To convert the etched depth to the sputtering yield, we assumed that the densities of Ta, Ta_2O_5, and TaN films used in our experiments were 16.69, 8.73, and 14.30 g/cm^3, respectively. The ion dose used for the measurement of sputtering yields in this study was in the range of 1×10^{17} to 3×10^{18} ions/cm^2. The chemical compositions of beam irradiated sample surfaces were also analyzed with *in-situ* x-ray photoelectron spectroscopy (XPS). The ion doses used for XPS observation were approximately 1×10^{17} ions/cm^2, at which the etching processes typically reached steady states.

III. EXPERIMENTAL RESULTS

A. Sputtering yields of Ta, Ta_2O_5, and TaN

The sputtering yields of Ta, Ta_2O_5, and TaN by energetic Ar^+, CO^+, and N^+ ions obtained from our beam experiments are summarized in Fig. 1. In all cases that show incident energy dependence, the sputtering yields are found to be nearly linear with the square root of the incident energy, as proposed by Steinbrüchel.[26] In Fig. 1(a), where sputtering yields of Ta, Ta_2O_5, and TaN by Ar^+ ions are given, the Ta yield is shown to be higher than that of Ta_2O_5 or TaN, indicating that the oxide or nitride of Ta has a lower sputtering yield and therefore is more resistant against physical sputtering. Differences of physical sputtering yields among these materials are consistent with bond dissociation energies (at a temperature of 298 K) of Ta–Ta, Ta–O, and Ta–N bonds, which are 390 ± 96, 839, and 607 ± 84 kJ/mol, respectively.[27] In general, the higher the bond energy of a material is, the lower its physical sputtering yield is for a given incident ion species and a given incident ion energy.

On the other hand, the Ta sputtering yields by CO^+ or N^+ ions are given in Fig. 1(b), all of which are significantly lower than their corresponding yields by Ar^+ ions. For

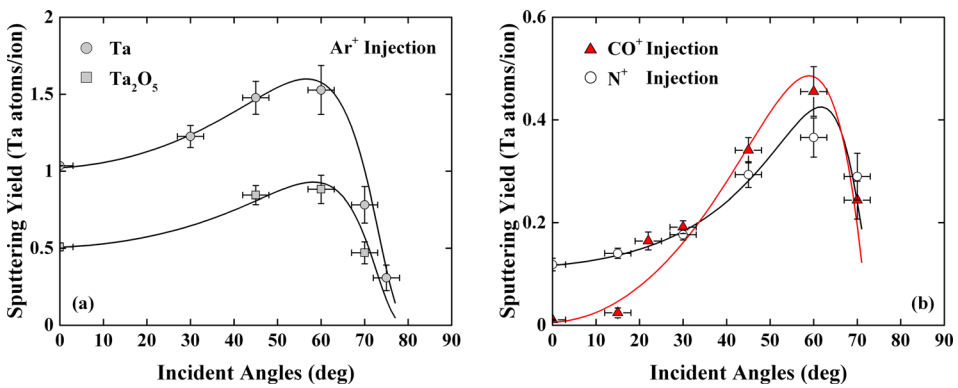

FIG. 2. (Color online) Dependence of the sputtering yields of (a) Ta and Ta_2O_5 by energetic Ar^+ ions and (b) Ta by energetic N^+ and CO^+ ions on the angle of ion incidence, measured from the surface normal. The incident ion energy is 1000 eV.

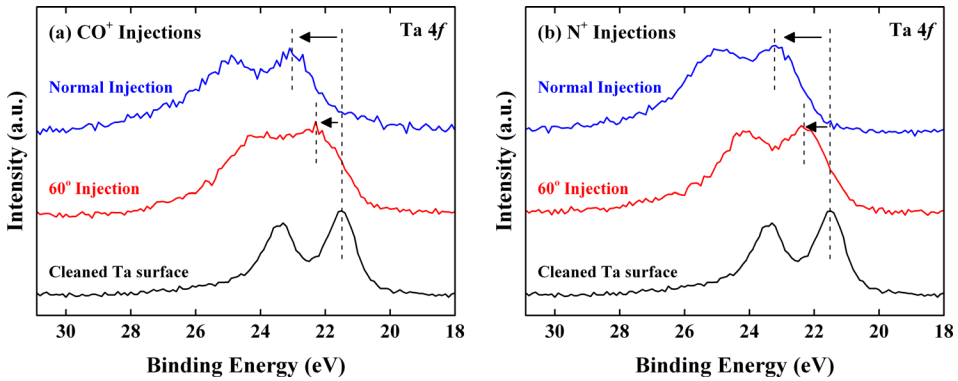

FIG. 3. (Color online) Ta 4*f* photoelectron spectra from XPS of Ta surfaces irradiated by (a) CO^+ and (b) N^+ ions. The binding energies of the observed lower-energy Ta peaks are 21.4 (clean Ta surface), 22.1 eV (CO^+ 60° injection), and 23.1 eV (CO^+ normal injection) in (a) and 22.3 eV (N^+ 60° injection) and 23.1 eV (N^+ normal injection) in (b). The ion incident energy is 1000 eV and the ion dose is approximately 1×10^{17} cm^2.

example, the sputtering yield of Ta by CO^+ ions is two-order-of-magnitude lower than that by Ar^+ ions. As we shall show in a moment, a suboxide or subnitride layer is simultaneously formed on the surface of Ta as it is etched by CO^+ or N^+ ions. The formation of such a suboxide or subnitride layer is likely to affect the sputtering yield.

B. Sputtering of Ta and Ta_2O_5 at oblique angles

Figure 2 shows the sputtering yields of Ta and Ta_2O_5 by Ar^+ ions in (a) and the sputtering yields of Ta by CO^+ and N^+ ions in (b) as functions of the ion incident angle, obtained from the beam experiments. The solid curves are the guides to the eye. The incident ion energy is 1000 eV. It is seen that the sputtering yields of Ta by Ar^+, CO^+, and N^+ ions and that of Ta_2O_5 by Ar^+ ions show typical and strong dependence on the angle of incidence, similar to those of other materials, as shown in, e.g., Ref. 28. The angle dependence of the sputtering yield of Ta by CO^+ ions is especially strong and, especially at around $\theta = 20°$, it exhibits a large gap. Details of the nature of sputtering yield of Ta by CO^+ ions around this angle of incidence will be discussed in a separate article.[29]

C. XPS analyses of Ta surfaces

To understand possible chemical reactions of Ta with incident CO^+ and N^+ ions, we have analyzed the chemical

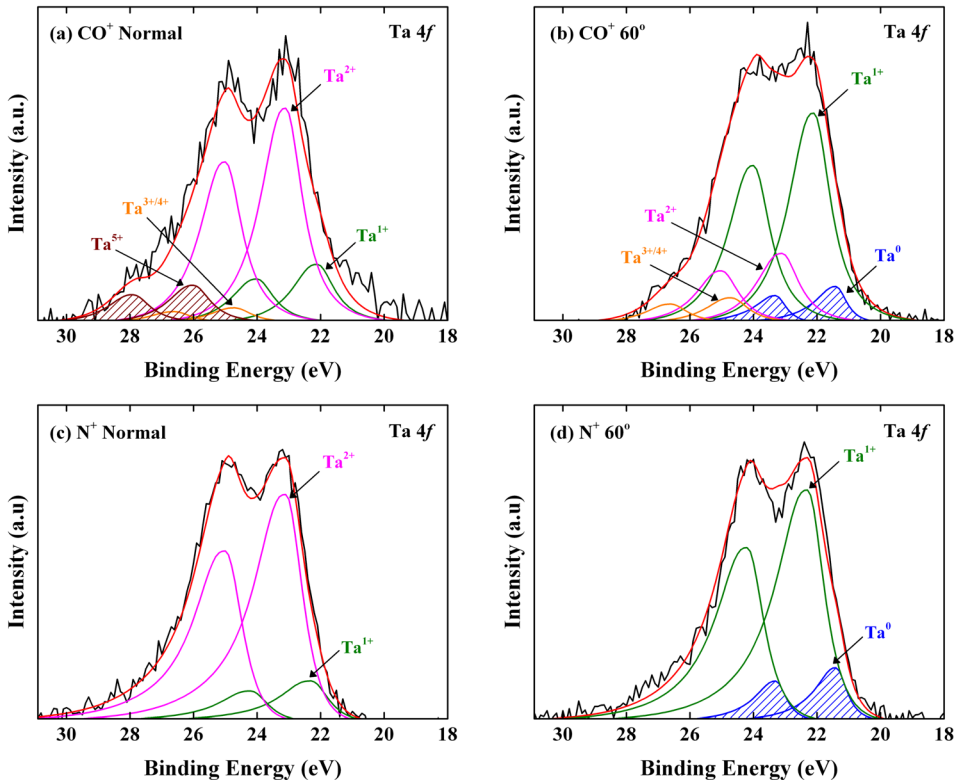

FIG. 4. (Color online) Decomposition of Ta 4*f* photoelectron spectra into different ionic states (i.e., oxidation states) of Ta. The spectra are obtained from XPS of Ta surfaces exposed to (a) normal ($\theta = 0°$) and (b) oblique ($\theta = 60°$) incidence of CO^+ ion beams and (c) normal and (d) oblique ($\theta = 60°$) incidence of N^+ ion beams, with θ being the angle of ion incidence. The ion incident energy is 1000 eV and the ion dose is approximately 1×10^{17} cm^2.

TABLE I. Binding energies and percentages of oxide states in Figs. 4(a) and 4(b).

Oxide states		Ta^0	Ta^{1+}	Ta^{2+}	$Ta^{3+/4+}$	Ta^{5+}
Binding energy (eV) $4f_{7/2}$		21.4	22.1	23.1	24.7	26.0
Percentage (%)	Normal injection	0	18	65.9	4.7	11.4
	60 deg injection	8.7	62.9	20.9	7.6	0

compositions of beam irradiated Ta surfaces by XPS. In this study, the background spectra were subtracted by the Shirley method and the Gaussian–Lorentzian functions with tail modifiers were used for curve fitting.

Figure 3 illustrates the changes in photoelectron spectra of the valence Ta 4*f* band of Ta films by CO^+ and N^+ ion injections. Here, the ion incident energy is 1000 eV and the angle of incident is either 0 (i.e., normal incidence) or 60°. The ion doses were in the range of 1×10^{17} ions/cm^2. It is seen that the spectra are shifted toward higher binding energies in both cases of CO^+ and N^+ ion injections. In each case, the largest chemical shift is observed in the case of normal ion incidence, meaning that the suboxide or subnitride layer formed on the Ta surface is closer to the normal oxide Ta_2O_5 or normal nitride TaN. We also note that, in the case of Fig. 3(a), TaC may also be formed together with the oxide. However, no carbon film accumulation that would reduce Ta signals at higher doses of CO^+ ions has been observed.

Figure 4 shows that the compositions of Ta ionic states were obtained from curve fitting to each photoelectron spectrum of the valence Ta 4*f* band. The binding energies for Ta^{1+}, Ta^{2+}, $Ta^{3+/4+}$, and Ta^{5+} have been selected to be sufficiently close to the data in earlier studies.[30–33] It is seen in Figs. 4(a) and 4(b) that the tantalum suboxide formed on Ta by CO^+ ions of normal incidence contains Ta having an oxidation state of 5 (i.e., Ta^{5+}), whereas that by CO^+ ions of oblique incidence contains more Ta of lower oxidation states. Especially metallic Ta (i.e., Ta^0) is seen in Fig. 4(b), which is the signal coming from the underlying Ta metal surface, implying that the suboxide film of Fig. 4(b) is thinner than that of Fig. 4(a). Similarly, it is seen in Figs. 4(c) and 4(d) that the subnitride formed on Ta by N^+ ions of normal incidence contains more Ta^{2+} than that by N^+ ions of oblique incidence. The fact that Ta^0 is seen in Fig. 4(d) also implies that the subnitride film of Fig. 4(d) is thinner than that of Fig. 4(c). Binding energies and percentages of oxides and nitrides in Fig. 4 obtained from curve fitting[33] are summarized in Tables I and II.

TABLE II. Binding energies and percentages of nitride states in Figs. 4(c) and 4(d).

Nitride states		Ta^0	Ta^{1+}	Ta^{2+}
Binding energy (eV) $4f_{7/2}$		21.4	22.3	23.1
Percentage (%)	Normal injection	0	15.1	84.9
	60 deg injection	13.4	86.6	0

IV. DISCUSSION AND CONCLUSIONS

In this study, we have shown that incidence of energetic CO^+ or N^+ ions on Ta forms a suboxide or subnitride layer on the Ta surface and there seems a correlation between the nature of the suboxide or subnitride film and its sputtering yield. In the measurement of the sputtering yields of Ta films as functions of the incidence angle θ, we have observed that, in both cases of CO^+ and N^+ ion incidence, the sputtering yield of Ta is higher at $\theta = 60°$ (i.e., oblique incidence) than that at $\theta = 0°$ (i.e., normal incidence) and the suboxide or subnitride formed on the Ta surface contains more Ta of higher oxidation states in the case of normal incidence than in the case of oblique incidence. The same XPS measurements also indicate that the suboxide or subnitride film is thicker in the case of normal incidence than in the case of oblique incidence.

These results suggest a correlation that the higher the oxidation state of Ta (i.e., integer n of Ta^{n+}) in the oxide or nitride film is, the lower its sputtering yield is. Especially, if the oxidation state of Ta is maintained to be higher (i.e., closer to its full value +5 for oxide and +3 for nitride) during the etching process by continuous supply of oxygen or nitrogen from incident ions, the sputtering yield of the tantalum oxide or nitride is smaller than that of suboxide or subnitride of Ta with lower oxidation states.

In this study, we observed the relation between the sputtering yield and chemical compositions of the beam irradiated Ta surface during angle-dependent sputtering processes of Ta by energetic CO^+ and N^+ ions. In these experiments, we could not separate the effects of oxidation state of Ta and the film thickness on the sputtering yield. For example, when the sputtering yield is higher, the oxidation state of Ta of the formed oxide or nitride film is lower and the film is also thinner. Figure 1 indicates that the sputtering yields of both TaO_x and TaN_x are lower than that of Ta and therefore TaO_x and TaN_x are considered to be more sputtering resistant than Ta. Therefore, both effects, i.e., the formation of a thicker oxide or nitride film and the higher oxidation states of Ta in it, are considered to contribute to the apparent low sputtering yield of Ta by energetic CO^+ or N^+ ions in the case of normal incidence than in the case of oblique incidence.

In summary, we have performed mass-selected ion beam experiments to evaluate the sputtering yields of Ta by CO^+ and N^+ ions and analyzed the chemical compositions of beam irradiated Ta surfaces by XPS. It has been observed that there seems a correlation between the sputtering yield and the chemical nature of the suboxide or subnitride on Ta, as discussed above. In the case of the normal incidence of CO^+ ions on a Ta film, a Ta_2O_5 layer is formed on the Ta film, which reduces the apparent Ta sputtering yield since Ta_2O_5 is harder to be physically sputtered by incident ions than metallic Ta. Similarly, in the case of the normal incidence of N^+ ions on a Ta film, a TaN layer is formed on the Ta film, which reduces the apparent sputtering yield of the Ta film since TaN is harder to be physically sputtered by incident ions than metallic Ta. Furthermore, when the angle of incidence increases from zero to 60°, the normal oxide or

nitride formation by incident CO^+ or N^+ ions is impeded and a suboxide or subnitride is formed instead. Such an angle-dependent formation of a suboxide or subnitride results in strong dependence of the Ta sputtering yield on the angle of incidence, which has been also observed in this study. Because of such strong angle dependence of the sputtering yield, a Ta mask typically exhibits strong faceting during etching processes. However, the analyses of this study suggest that, if the oxidation or nitridation of a Ta mask surface is continuously promoted by some means, the mask faceting during the etching process may be minimized.

ACKNOWLEDGMENTS

The authors would like to thank Makoto Satake of Hitachi, Ltd. for his helpful discussion. This work was partially supported by Grants-in-Aid for Scientific Research from the Ministry of Education, Culture, Sports, Science and Technology of Japan.

[1]W. J. Gallagher *et al*., J. Appl. Phys. **81**, 3741 (1997).
[2]T. Miyazaki, S. Kumagai, and T. Yaoi, J. Appl. Phys. **81**, 3753 (1997).
[3]S. Tehrani, J. M. Slaughter, E. Chen, M. Durlam, J. Shi, and M. DeHerrera, IEEE Trans. Magn. **35**, 2814 (1999).
[4]S. Tehrani *et al*., IEEE Trans Magn. **36**, 2752 (2000).
[5]M. G. J. Heijman, Plasma Chem. Plasma Process. **8**, 383 (1988).
[6]K. B. Jung *et al*., J, Appl. Phys. **85**, 4788 (1999).
[7]T. Kim, J. K. Chen, and J. P. Chang: J. Vac. Sci. Technol. A **32**, 041305 (2014).
[8]T. Kim, Y. Kim, J. K. Chen, and J. P. Chang, J. Vac. Sci. Technol. A **33**, 021308 (2015).
[9]I. Nakatani, IEEE Trans. Magn. **32**, 4448 (1996).
[10]N. Matsui, K. Mashimo, A. Egami, A. Konishi, O. Okada, and T. Tsukada, Vacuum **66**, 472 (2002).
[11]H. Kubota, K. Ueda, Y. Ando, and T. Miyazaki, J. Magn. Magn. Mater. **272**, E1421 (2004).
[12]X. Kong, D. Krása, H. P. Zhou, W. Williams, S. McVitie, J. M. R. Weaver, and C. D. W. Wilkinson, Microelectron. Eng. **85**, 988 (2008).
[13]J. Y. Park, S. K. Kang, M. H. Jeon, M. S. Jhon, and G. Y. Yeom, J. Electrochem. Soc. **158**, H1 (2011).
[14]M. H. Jeon, H. J. Kim, K. C. Yang, S. K. Kang, K. N. Kim, and G. Y. Yeom, Jpn. J. Appl. Phys. **52**, 05EB03 (2013).
[15]T. Osada, M. Doi, K. Sakamoto, H. Maehara, and Y. Kodaira, *Proceedings of the 26th Symposium Dry Process (DPS)* (2004), p. 127.
[16]K. Kinoshita, H. Utsumi, K. Suemitsu, H. Hada, and T. Sugibayashi, Jpn. J. Appl. Phys. **49**, 08JB02 (2010).
[17]E. H. Kim, T. Y. Lee, and C. W. Chung, J. Electrochem. Soc. **159**, H230 (2012).
[18]K. Ishikawa, K. Karahashi, H. Tsuboi, K. Yanai, and M. Nakamura, J. Vac. Sci. Technol. A **21**, L1 (2003).
[19]K. Karahashi, K. Yanai, K. Ishikawa, H. Tsuboi, K. Kurihara, and M. Nakamura: J. Vac. Sci. Technol. A **22**, 1166 (2004).
[20]K. Yanai, K. Karahashi, K. Ishikawa, and M. Nakamura, J. Appl. Phys. **97**, 053302 (2005).
[21]T. Ito, K. Karahashi, M. Fukasawa, T. Tatsumi1, and S. Hamaguchi, Jpn. J. Appl. Phys. **50**, 08KD02 (2011).
[22]T. Ito, K. Karahashi, M. Fukasawa, T. Tatsumi, and S. Hamaguchi, J. Vac. Sci. Technol. A **29**, 050601 (2011).
[23]T. Ito, K. Karahashi, K. Mizotani, M. Isobe, S.-Y. Kang, M. Honda, and S. Hamaguchi, Jpn. J. Appl. Phys. **51**, 08HB01 (2012).
[24]T. Ito, K. Karahashi, S.-Y. Kang, and S. Hamaguchi, J. Vac. Sci. Technol. A **31**, 031301 (2013).
[25]K. Karahashi and S. Hamaguchi, J. Phys. D: Appl. Phys. **47**, 224008 (2014).
[26]C. Steinbrüchel, Appl. Phys. Lett. **55**, 1960 (1989).
[27]*CRC Handbook of Chemistry and Physics*, 91st ed., edited by W. M. Haynes (Taylor and Francis Group, Boca Raton, FL, 2010–2011).
[28]R. E. Lee, J. Vac. Sci. Technol. **61**, 164 (1979).
[29]M. Satake, M. Yamada, H. Li, K. Karahashi, and S. Hamaguchi, "Change in dry etching resistance of Ta with an oxidation state of surface oxide layer," J. Vac. Soc. Technol. B (submitted).
[30]E. Atanassova, T. Dimitrova, and J. Koprinarova, Appl. Surf. Sci. **84**, 193 (1995).
[31]V. J. Tu, J. Y. Jeong, A. Schütze, S. E. Babayan, G. Ding, G. S. Selwyn, and R. F. Hicks, J. Vac. Sci. Technol. A **18**, 2799 (2000).
[32]A. Arranz and C. Palacio, Appl. Phys. A **81**, 1405 (2005).
[33]M. V. Ivanov, T. V. Perevalov, V. S. Aliev, V. A. Gritsenko, and V. V. Kaichev, J. Appl. Phys. **110**, 024115 (2011).